World Academy of Science, Engineering and Technology
International Journal of Materials and Metallurgical Engineering
Vol:9, No:3, 2015

Evaluation of Corrosion by Impedance Spectroscopy of Embedded Steel in an Alternative Concrete Exposed to the Chloride Ion

Erika J. Ruíz, Jairo R. Cortes, Willian A. Aperador

***Abstract*—**In this article was evaluated the protective effect of the alternative concrete obtained from the binary mixture of fly ash, and iron and steel slag. After mixing the cement with aggregates, structural steel was inserted in the matrix cementitious. The study was conducted comparatively with specimens exposed to natural conditions free of chloride ion. The chloride ion effect on the specimens accelerated under controlled conditions (3.5% NaCl and 25°C temperature). The impedance data were acquired in a range of 1 mHz to 100 kHz.

***Keywords*—**Alternative concrete, corrosion, alkaline activation.

I. Introduction

IN recent years, the use of by-products and industrial waste such as fly-ash, silica fume, steel slag furnace among others, has acquired importance, due to the fundamental search of energy savings and the reducing consumption of natural resources. Therefore, the industry cement has ventured into the development and production of new types of alternative cements [1], [2]. Among these materials known as supplemental or additions, they are the fly ash (FA) and granulated blast-furnace slag (GBFS), which have been used successfully as a partial and total substitute for the cement ordinary Portland within of the mixtures concrete, giving place to materials with best performances mechanical and durability. The EIS technique was first applied in the evaluation of the corrosion of steel embedded in concrete in the early 90s and today is considered very useful for understanding the behavior of the system steel/concrete [3]-[6].

This paper reports the electrochemical properties obtained of a steel embedded in concrete mixtures of steel slag and fly ash, when it is subjected to normal atmospheric conditions and environments with high concentrations of CO2. The measurements of electrochemical impedance spectroscopy were performed at different times of exposure.

II. Experimental Method

A. Fly Ash Type 8 (C)

The fly ash was obtained from the Termopaipa thermoelectric plant, whose chemical composition is recorded in Table I. The loss on ignition was 6.54% of the total mass determined by calcination of the sample at 1000°C, this value is associated mainly to the unburned carbon remnants. Additionally, it was evaluated the reactive of the fly ash silica percentage, following the procedure described in the standard UNE 80-225-93, obtaining a value of 46.15% in mass.

Erika J. Ruiz, Jairo R. Cortes, and W. Aperador are with the School of Engineering, Universidad Militar Nueva Granada, Carrera 11 No. 101-80, Bogotá, Colombia (phone: +57-1-6500000; e-mail: erika.ruiz@unimilitar.edu.co, jairo.cortes@unimilitar.edu.co, g.ing.materiales@gmail.com).

B. Granulated Blast Furnace Slag (GBFS)

Table I shows the chemical composition, ratios basicity ($CaO + MgO / SiO_2 + Al_2O_3$) of 1 and quality 1.0 ($CaO + MgO + Al_2O_3 / SiO_2 + TiO_2$) of 1.73. A solution of sodium silicate at a concentration of 5%of Na2O expressed as percent in weight slag (ASTM C 989-99) was used as alkaline activator.

TABLE I
Chemical Composition of Fly Ash, Steel Slag

Compound	Fly Ash (% in mass)	Granulated Blast-furnace Slag (% in mass)
SiO_2	54.3	33.7
Al_2O_3	22.8	12.8
Fe_2O_3	5.8	0.48
CaO	6.9	45.4
MgO	0.8	1
Na_2O	0.9	0.12
K_2O	1.7	1.5
P_2O_5	0.7	
TiO_2	1.6	0.5
MnO	0.01	-
SO_3	0.92	-
SiO_2/Al_2O_3	3.5	2.63
Fe_2O_3	22.8	12.8

For the study, three types of concrete specimens were conformed: 100% granulated blast furnace slag (GBFS), 100% alkali activated fly ash, and 50% of both additions, activated slag and fly ash (C), as is shown in the Table II.

TABLE II
Type and Conformation of Concrete Specimens

Class	Composition
G100	100% GBFS
FA100	100% fly ash
G50-FA50	50% of GBFS + 50% of fly ash

C. Electrochemical Test

The electrochemical characterization was performed by a potentiostat / galvanostat Gamry model PCI 4 applying the electrochemical impedance spectroscopy technique, using a

electrochemical cell composed by a counter electrode of graphite, a reference electrode Ag/AgCl and as a working electrode was used the structural steel ASTM A 706 with an exposed area of 10 cm^2. All the electrochemical tests were performed in a solution with 3.5% NaCl for 6 and 12 months of exposure. Fig. 1 shows the schematic diagram of the test assembly. The measurements of the concretes exposed to the natural environment were performed at the same exposure ages. The Nyquist diagrams were obtained by performing frequency sweeps in the range of 100 kHz to 0.001 Hz using a sinusoidal signal with an amplitude of 10 mV

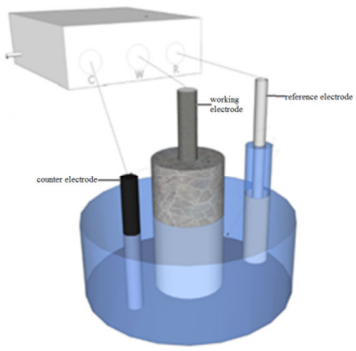

Fig. 1 Experimental setup for performing electrochemical measurements

III. Results and Discussions

A. Exposure in Natural Environment

In the case of the concrete exposed to natural environment was obtained the graphs presented in Fig. 3; are associated the circuits included in Fig. 2, for all levels evaluated.

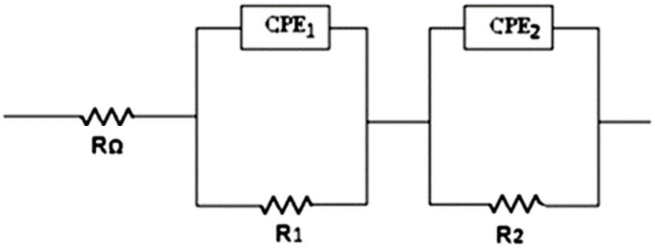

Fig. 2 Equivalent circuit of the activated concrete exposed to chloride ion

The circuit of Fig. 2 is the most common in the study of systems involving concrete, this model is found in various jobs, including that of [7]. The resistance Rc + s corresponds the domain to high frequency (between 1 kHz and 100 kHz) and is related to the electrical resistance of the concrete, including electrolyte resistance (The resistance of electrolyte is negligible compared to the strength of concrete). Rc + s may also include contributions from the effects of the cover that is the interface between the electrolyte and the concrete [8]-[11]. The resistor R1 corresponds to the domain intermediate frequency (1 kHz at 50Hz), and is used to represent the resistance in the transition zone. The CPE1 corresponds to the representation capacitance of non-ideal in the zone of the transition area interface cement / aggregate near the pore [12]. The dominance of low frequency (50Hz to 1mHz) is used to evaluate the process of charge transfer along with the mass transport process [13], [14] and usually corresponds to the resistance Rp; CPE2 is used to determine the capacitance non-ideal steel surface [14].

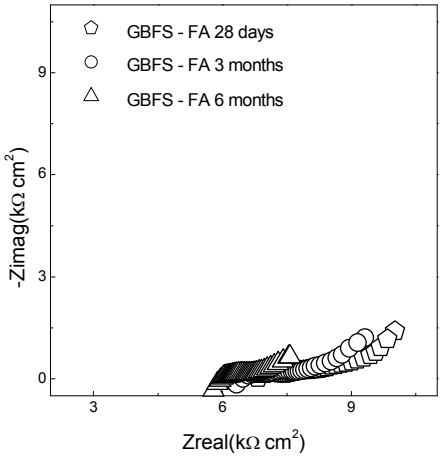

Fig. 3 Nyquist diagrams corresponding to the concrete alternative exposed to natural environment

B. Chloride Exposure

The impedance spectroscopy technique that was applied to alternative concrete is adjusted to a physical model (Fig. 2), which depends on both evaluated states.

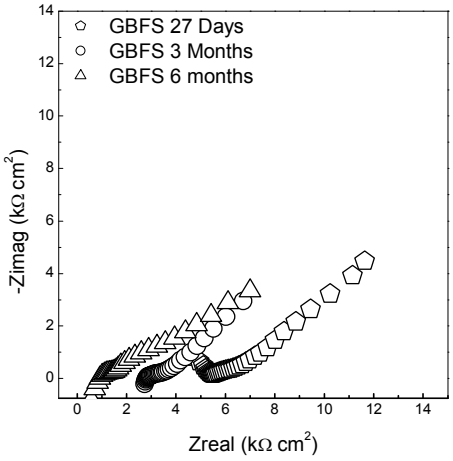

Fig. 4 Nyquist plot corresponding the concrete alternative exposed chloride ion

For the concrete in contact with the chloride ion was found at high frequencies, a first resistance (Rc + s) associated to the concrete pore solution; then a CPE and a resistance were found, these elements are related to the elements on the outside the concrete, due to the generated reactions or the surface absorption of some of the species with chloride ion, at the domain of lower frequencies; normally, a transfer process of the charge mass is found, it corresponds to the last R and CPE, these elements are located in the corresponding interface

area of the concrete and steel.

C. Scanning Electron Microscopy

An effective way to study the corrosion of steel in each of the concrete types is to study the morphology of the products generated (oxides and hydroxides) during the time when they were under attack by chloride ions. This complements the information obtained through electrochemical field or laboratory techniques. By observing the surface of the steel, which was embedded in each concrete type, therefore, at low magnification the presented attack type can be inferred. At higher magnifications, it is possible to determine the type of generated oxide.

The steel embedded in concrete GBFS subjected to aggressive conditions apparently showed a homogeneous distribution of the corrosion products (Fig. 5). It can be noted as this oxide layer is not on the entire surface of the metal. This matches the electrochemical data obtained at the end of the study, because although stable resistance values presented on the polarization versus time, were not high enough due to the formation of non-uniform oxide layers. Chloride ions break the oxide layer so that a porous surface was generated, which no protects the steel underneath. This is why the polarization resistance has low values for these systems.

Fig. 5 Surface of steel embedded in concrete GBFS subjected to chloride ions

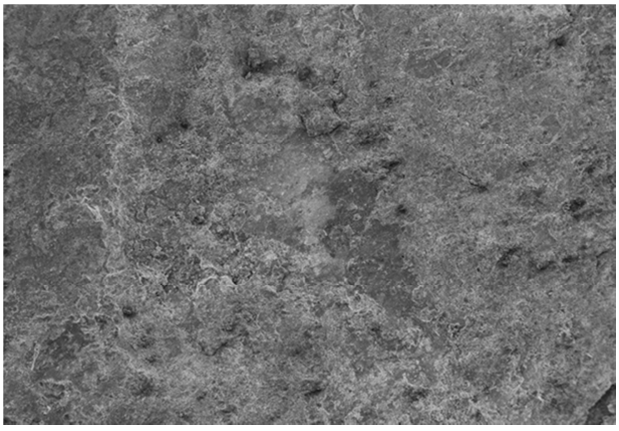

Fig. 6 Surface steel embedded in fly ash concrete, subjected to chloride attack

Passivity conditions found in steel electrochemically, which was embedded in concrete based on fly ash are explained by observing the final surface by scanning electron microscopy. At first, the metal has low protection against corrosive attack (Fig 6), since a very small amount is displayed oxide. This demonstrates the stability of the protective layer of steel under stable environmental conditions reflected in the high polarization resistance in these systems.

D. Concrete Steel Interface

Apart from analyzed surface other specimen was prepared for study by electron microscopy. In this case, a cross-section was obtained to study the state of the interface between each type of concrete and the reinforcing steel. Nevertheless, observing the interface formed between the metal reinforcement and the ceramic matrix based activated slag was evidence the difference between each item. Unlike its counterpart fly ash, concrete GBFS subjected to the same conditions presents a homogeneous oxide layer on steel, at least in terms of its thickness. Slag concrete also shows some cracks inside, but their size and distribution is much lower than those presented in the fly ash.

IV. Conclusions

The improved protection mechanism of the iron and steel slag concrete provides to the metal a uniform oxide layer thereon. The passivation method may be caused by the absence of cracks in concrete that prevents passage of noxious substances which destabilize the oxide coating and create corrosion. This fact shows that low values of resistance to polarization in the fly ash is generated by the simultaneous combination of the formation of protective layers and slightly decreasing the restricting the passage of noxious elements to the system.

Acknowledgment

This research was supported by "Vicerrectoría de investigaciones de la Universidad Militar Nueva Granada" under contract ING 1572.

References

[1] W. Aperador, R. Mejía de Gutiérrez, D.M. Bastidas, “Steel corrosion behaviour in carbonated alkali-activated slag concrete” Corrosion Science., Vol 51, no. 9, pp. 2027-2033, Sep. 2009.

[2] M. Criado, D.M. Bastidas, S. Fajardo, A. Fernández-Jiménez, J.M. Bastidas, “Corrosion behaviour of a new low-nickel stainless steel embedded in activated fly ash mortars” Cement and Concrete Composites., Vol 33, no 6, pp. 644-652, July 2011.

[3] M. Criado, C. Monticelli, S. Fajardo, D. Gelli, V. Grassi, J.M. Bastidas, “Organic corrosion inhibitor mixtures for reinforcing steel embedded in carbonated alkali-activated fly ash mortar”, Construction and Building Materials., Vol 35, pp. 30-37, 2012.

[4] S. Gavela, A. Ntziouni, E. Rakanta, N. Kouloumbi, V. Kasselouri-Rigopoulou, “Corrosion behaviour of steel rebars in reinforced concrete containing thermoplastic wastes as aggregates”, Construction and Building Materials., Vol 41, pp. 419-426, April 2013.

[5] M. Torres-Luque, E. Bastidas-Arteaga, F. Schoefs, M. Sánchez-Silva, J.F. Osma, “Non-destructive methods for measuring chloride ingress into concrete: State-of-the-art and future challenges”, Construction and Building Materials., Vol 68, pp. 68-81, Oct. 2014.

[6] A.A. Sagüés, M.A. Pech-Canul, A.K.M. Shahid Al-Mansur, "Corrosion macrocell behavior of reinforcing steel in partially submerged concrete columns"., Corrosion Science., Vol 45, no 1,pp. 7-32, Jan. 2003,
[7] M. Criado, I. García-Díaz, J.M. Bastidas, F.J. Alguacil, F.A. López, C. Monticelli, "Effect of recycled glass fiber on the corrosion behavior of reinforced mortar", Construction and Building Materials., Vol 64, pp. 261-269, August 2014.
[8] I. Martínez, C. Andrade, "Application of EIS to cathodically protected steel: Tests in sodium chloride solution and in chloride contaminated concrete", Corrosion Science., Vol 50, no. 10, pp. 2948-2958, Oct. 2008.
[9] S. Fajardo, D.M. Bastidas, M. Criado, M. Romero, J.M. Bastidas, "Corrosion behaviour of a new low-nickel stainless steel in saturated calcium hydroxide solution", Construction and Building Materials, Vol. 25, no. 11, pp. 4190-4196. Nov. 2011.
[10] S.M. Alvarez, A. Bautista, F. Velasco, Corrosion behaviour of corrugated lean duplex stainless steels in simulated concrete pore solutions, Corrosion Science., Vol 53, no. 5, pp. 1748-1755, May 2011.
[11] J.J. Shi, W. Sun, "Effects of phosphate on the chloride-induced corrosion behavior of reinforcing steel in mortars", Cement and Concrete Composites, Vol 45, no. 1, pp. 166-175, Jan. 2014.
[12] C. Monticelli, M. Criado, S. Fajardo, J.M. Bastidas, M. Abbottoni, A. Balbo, "Corrosion behaviour of a Low Ni austenitic stainless steel in carbonated chloride-polluted alkali-activated fly ash mortar", Cement and Concrete Research., Vol 55, no1. pp. 49-58, Jan 2014.
[13] A. Shah, Y. Ribakov, "Recent trends in steel fibered high-strength concrete" Materials & Design, Vol. 32, no. 8–9, pp. 4122-4151, Sept. 2011
[14] A. Poursaee, C.M. Hansson, "Potential pitfalls in assessing chloride-induced corrosion of steel in concrete", Cement and Concrete Research, Vol. 39, no. 5, pp. 391-400, May 2009.